The EMBO Journal vol.12 no.8 pp.3017-3022, 1993

Agonist-induced localized Ca^{2+} spikes directly triggering exocytotic secretion in exocrine pancreas

Yoshio Maruyama, Gen Inooka, Yue Xin Li[1], Yasushi Miyashita[1] and Haruo Kasai[1,2]

Department of Physiology, Jichi Medical School, Minamikawachimachi 3311-1, Tochigi, 329-04 and [1]Department of Physiology, University of Tokyo, Hongo 7-3-1, Bunkyo-ku, 113 Japan

[2]Corresponding author

Communicated by E.Neher

We investigated how agonist-induced patterned rises in cytosolic Ca^{2+} concentration ($[Ca^{2+}]_i$) regulate exocytotic secretion in the rat pancreatic acinar cell. The distribution of $[Ca^{2+}]_i$ was visualized with a confocal microscope, which revealed that a Ca^{2+} ionophore, A23187, induced slow and homogeneous $[Ca^{2+}]_i$ rises, while acetylcholine (ACh) always triggered primary Ca^{2+} spikes at the granular area which bears secretory granules. Secretion was monitored by measuring capacitance with the patch clamp method. Errors in the estimates of membrane capacitance (C) due to changes in conductance (G) were experimentally as well as theoretically evaluated to be one-tenth of the actual signals. We found that A23187 raised G without changing C at a low concentration, while it triggered asynchronous rises in G and C with lags in C, at a high concentration. By contrast, ACh triggered simultaneous rapid rises in G and C. Our results support the hypothesis that exocytotic secretion is less sensitive to Ca^{2+} than to ion channels and is directly caused by agonist-induced primary Ca^{2+} spikes at the granular area. It is therefore suggested that spatio-temporal patterns of Ca^{2+} oscillations could play a key role in exocytotic secretion from the exocrine acinar cell.

Key words: Ca^{2+}/capacitance measurement/confocal microscope/imaging/patch clamp/secretion

Introduction

The recent advent of Ca^{2+} indicator dyes and Ca^{2+} imaging techniques has made it possible to unveil the dynamic changes in cytosolic calcium concentration ($[Ca^{2+}]_i$) induced by agonists in various cells. The $[Ca^{2+}]_i$ rises often take the form of a wave and often oscillate during lasting stimulation by agonists (Berridge, 1993). The patterned Ca^{2+} rises are in most cases mediated through the opening of Ca^{2+} release channels that are regulated by second messengers, such as inositol 1,4,5-trisphosphate and Ca^{2+}. The presence of many examples of such dynamic $[Ca^{2+}]_i$ changes and the ongoing elucidation of underlying molecular mechanisms have led us to hypothesize that the patterned $[Ca^{2+}]_i$ rise may play important roles in cellular functions (Berridge, 1993). Indeed, in some cases the role of these dynamic Ca^{2+} changes has progressed well beyond the realm of hypothesis (Kasai and Augustine, 1990; Brundage *et al.*, 1991). One example is the rat pancreatic acinar cell, where agonists first trigger a $[Ca^{2+}]_i$ rise at the luminal pole and subsequently induce Ca^{2+} waves which propagate towards the basal pole (Kasai and Augustine, 1990; Nathanson *et al.*, 1992; Toescu *et al.*, 1992). The sequence of increases in $[Ca^{2+}]_i$ and its oscillatory appearance have been implicated in the patterned activation of ion channels and in unidirectional fluid secretion from the acinus (Kasai and Augustine, 1990).

In the present paper, we have further addressed whether the characteristic pattern of increases in $[Ca^{2+}]_i$ governs the fusion of secretory granules in the pancreatic acinar cell. To answer this question, we have visualized the distribution of $[Ca^{2+}]_i$, and monitored changes in membrane capacitance reflecting vesicular fusion, while stimulating the cells either with an agonist, acetylcholine (ACh), or with a Ca^{2+}-ionophore, A23187. This is because previous authors have reported that these two stimuli give rise to different patterns of secretory fusion as well as different patterns of $[Ca^{2+}]_i$ increases (Maruyama, 1988; Toescu *et al.*, 1992). In the present study, we compared the results of Ca^{2+} imaging and capacitance measurement in a more quantitative manner to find out the correlation between $[Ca^{2+}]_i$ increases and secretion. We have also improved the reliability of techniques for measuring $[Ca^{2+}]_i$ distribution and membrane capacitance: the confocal laser scanning microscope used to visualize patterned $[Ca^{2+}]_i$ increases had a resolution which could capture increases in $[Ca^{2+}]_i$ in the vicinity of secretory granules.

The reliability of the measurement of capacitance has also been improved. The major difficulty with measuring capacitance in the exocrine cells lies in the fact that agonists tend to induce simultaneous fusion of secretory granules and activation of ion channels (Maruyama, 1988, 1989c). Hence, the estimation of membrane capacitance (C) might be affected by large changes in membrane conductance (G). In the present study, the cross-talk between the estimates of C and G was estimated experimentally using lacrimal gland cells. We also theoretically evaluated the errors. Both of the results confirmed that the errors were not significant. The clear differences in changes in C evoked with ACh and with A23187 were therefore interpreted as reflecting actual differences in their effects on exocytotic secretion. We found that differences in secretion evoked by ACh or A23187 could be accounted for by the distinctive spatio-temporal patterns of $[Ca^{2+}]_i$ rises associated with the two stimuli.

Results

Spatio-temporal patterns of $[Ca^{2+}]_i$ rises induced with A23187 and ACh

We first examined the effects of a Ca^{2+} ionophore, A23187, on the distribution of $[Ca^{2+}]_i$ in pancreatic acinar cells. When the concentration of A23187 was 0.2 μM, $[Ca^{2+}]_i$ rose very slowly and did not reach 0.3 μM (n = 4, Table I), while large increases in $[Ca^{2+}]_i$ were detected

Table I. Amplitudes and lags in ΔC and $[Ca^{2+}]_i$ induced by A23187 and ACh

	Maximum ΔC ±SD (fF)	Lag in ΔC ±SD (s)	*n*	Maximum $[Ca^{2+}]_i$ ±SD (μM)	Lag in $[Ca^{2+}]_i$ rises ±SD (s)	*n*
A23187 0.2 μM	20 ± 5	∞	4	0.23 ± 0.1	∞	3
A23187 1 μM	1400 ± 663	4.8 ± 2.4	6	>0.9	6 ± 3	5
A23187 1 μM[a]	280 ± 120	33 ± 18	4	0.68 ± 0.15	30 ± 10	4
ACh 0.5 μM	312 ± 146	<0.1 s	9	0.76 ± 0.12	0.4 ± 0.2	8
ACh 0.5 μM (Ca^{2+}-free)[b]	246 ± 140	<0.1 s	4	0.74 ± 0.13	0.4 ± 0.3	3

The lag in ΔC is defined as the time between the onset of rises in G and in C. The lag in $[Ca^{2+}]_i$ is the time required for $[Ca^{2+}]_i$ to rise from 0.2 to 0.4 μM in the granular area where increases in $[Ca^{2+}]_i$ were initiated.
[a]Cells were immersed in a Ca^{2+}-free external solution containing 0.5 mM EGTA for 5−10 min and stimulated with A23187 plus 1 mM Ca^{2+}.
[b]Cells were immersed in the control Ca^{2+}-containing solution, then stimulated with ACh together with 3 mM EGTA.

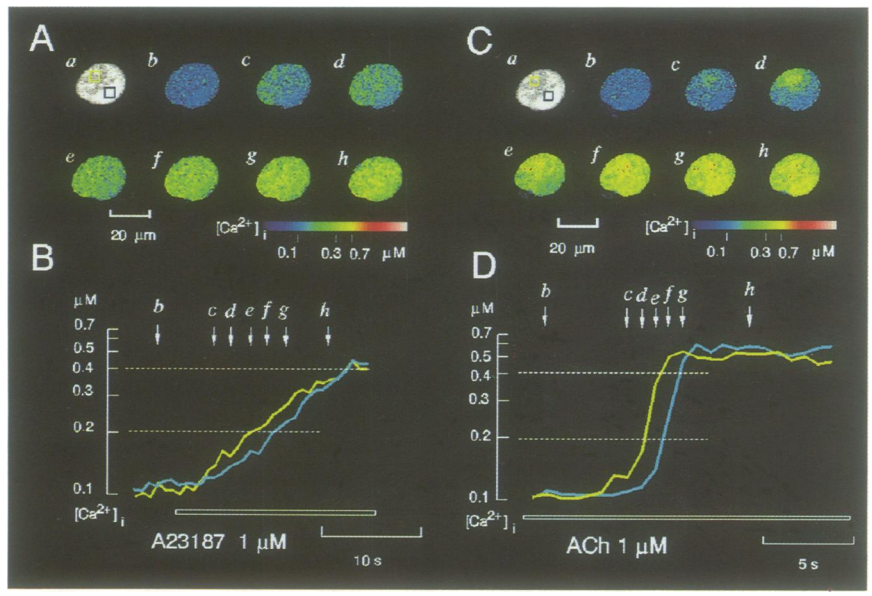

Fig. 1. Distribution of $[Ca^{2+}]_i$ in a single pancreatic acinar cell studied with a confocal laser scanning microscope. (**A**) and (**C**) Ca^{2+} images acquired from the same cell stimulated either with A23187 (1 μM) or with ACh (1 μM), respectively. Image a shows an epifluorescent view of the acinar cell. Images b−h show estimated $[Ca^{2+}]_i$ represented by the indicated pseudocolour scaling. Averaged $[Ca^{2+}]_i$ within the rectangles in image a in (A) and (C) are plotted versus time in (**B**) and (**D**), respectively. Each coloured line represents averaged $[Ca^{2+}]_i$ from the rectangles with the corresponding colours in (a). Arrows indicate time points when $[Ca^{2+}]_i$ images b−h were acquired.

throughout the cells following treatment with 1 μM A23187 (Figure 1A, image b). To quantify the speed of increases in $[Ca^{2+}]_i$, the time lags required for $[Ca^{2+}]_i$ to rise from 0.2 μM to 0.4 μM was graphically obtained as shown in Figure 1B. The lags ranged from 4 to 13 s (Table I). It was often noticed that $[Ca^{2+}]_i$ was slightly higher in that part of the cell which was closest to the A23187 pipette (Figure 1A, image d, and yellow line in Figure 1B), suggesting that the incorporation of A23187 into the plasma membrane is related to the flow of drug application.

In contrast, the rises in $[Ca^{2+}]_i$ induced with ACh initially occurred in a small area within the granular area, and then sequentially spread towards the other parts of the granular area (Figure 1C, image e) and the basal area (Figure 1C, image f). The pattern of ACh-induced $[Ca^{2+}]_i$ increase never depended on the position of the application pipette. The $[Ca^{2+}]_i$ increase at the granular area was always fast (Figure 1D). The lags were 0.3−0.6 s for 0.5 μM ACh (Table I). This lag is significantly shorter than that, ~1 s, reported with conventional Ca^{2+} imaging (Kasai and Augustine, 1990; Toescu *et al.*, 1992), presumably due to sharp focusing of confocal optics to the plane where Ca^{2+} is actively released.

Separation of C and G in the capacitance measurements

In order to evaluate experimentally any errors in the measurement of capacitance (C) caused by the increases in conductance (G), we turned to lacrimal gland cells. These cells have Ca^{2+}-activated K^+-channels that are also activated simply by depolarization even at a resting $[Ca^{2+}]_i$ level (Findlay, 1984; Trautmann and Marty, 1984). Figure 2A shows a record of changes in C (ΔC) and G (ΔG), and current (I) in a single lacrimal acinar cell at various potentials (V). As measured with our system, the depolarization induces increases in outward currents and G, while it only slightly reduces C. The slight reductions in C represent errors due to large changes in G, since no changes in C could be detected in pancreatic acinar cells, which do not have such voltage-dependent K^+ conductance, following similar depolarization (Maruyama, 1988; Petersen, 1992). The values of ΔC for the four separate experiments

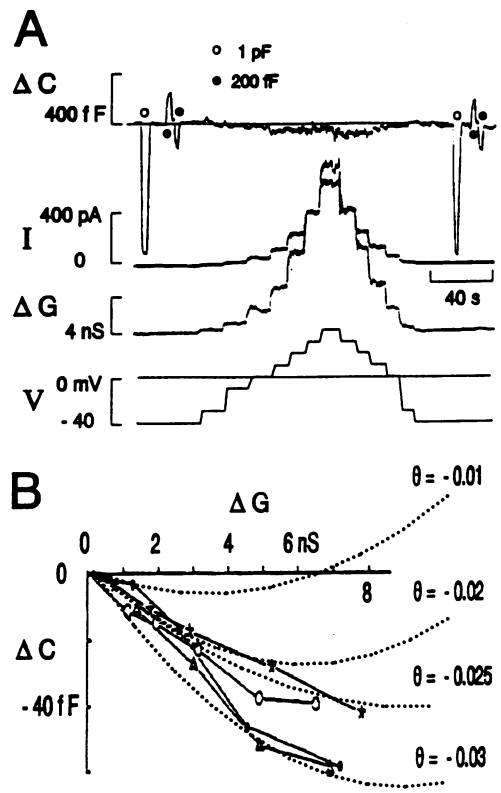

Fig. 2. Errors in the estimates of C caused by large changes in G during capacitance measurements in lacrimal acinar cells. (**A**) Apparent changes in membrane capacitance (ΔC), and conductance (ΔG) during step depolarization to various potentials (V). A current trace (I) was low-pass filtered at 40 Hz. Circles at the ΔC trace are calibration signals applied from a capacitance cancellation trimmer with an amplitude of 1 pF (open circle) or 200 fF (closed circle). (**B**) Relationship between apparent ΔG and ΔC obtained from four different experiments. Dotted lines show the errors predicted from equation 1 (see Discussion) with an error in the phase offset (θ) of −0.01, −0.02, −0.025 or −0.03 as indicated.

are plotted against ΔG in Figure 2B. The errors increase linearly up to a ΔG of 6 nS, where ΔC reaches 40 fF. These errors are about one-tenth of the actual changes in C in pancreatic acinar cells (Figures 2−4) and are considered negligible. In the lacrimal gland cells, on the other hand, large Ca^{2+}-activated K currents during stimulation (>10 nS) render the capacitance measurement less reliable.

Capacitance changes induced by A23187

We next investigated changes in capacitance in pancreatic acinar cells exposed to A23187, which homogeneously raises $[Ca^{2+}]_i$ throughout the cells (Figure 1A). At a low concentration (0.2 μM), A23187 raised only G without affecting C (n = 5; Figure 3A), but at a high concentration (1 μM), A23187 triggered increases in both G and C (Figure 3B and C), suggesting that exocytotic fusion is less sensitive to Ca^{2+} than Ca^{2+}-dependent ion channels. In addition, the rises in C lagged behind the rises in G. The lag was particularly notable when cells were exposed to A23187 in a Ca^{2+}-free solution (Figure 3B, Table I). The delay in increases in C could be due to the slowness in the application of A23187, which then slowed the time course of the rise in $[Ca^{2+}]_i$; when we applied A23187 through pipettes with particularly large openings (~30 μm), the responses of G and C became faster and the delay in C disappeared (Figure 3D).

Capacitance changes induced by ACh

As reported previously (Maruyama, 1988), ACh evoked synchronous changes in C and G in the Ca^{2+}-containing solution (Figure 2A). The rises in both C and G must require rises in $[Ca^{2+}]_i$, because these changes were abolished in cells (n = 4) internally dialysed with the pipette solution containing 3 mM EGTA. As expected from the imaging results, the rises in G and C triggered by ACh application were more rapid than those induced with A23187. The similarity in the time courses of changes in C and G tempted us to suspect that the rises in C might result from errors due to large increases in G. The results in a Ca^{2+}-free solution, however, ruled out this possibility; the recovery in rises in C was dramatically delayed (Figure 4B), and a large dissociation between G and C appeared after G recovered to the base line (Maruyama, 1989a). A similar delay in the recovery of C was detected with A23187 stimulation (Figure 3B). Thus, it appears that endocytosis in exocrine cells depends on external Ca^{2+} (Maruyama, 1989a). This dependence is not due to chronic changes in the properties of acinar cells immersed in Ca^{2+}-free solution for a long time, because similar delays in the recovery of increases in C were also observed following application of ACh together with EGTA in the Ca^{2+}-containing solution (n = 5; Figure 2C). Large jumps in C in the recovery phase were detected only in two out of five cells examined (Figure 4B and C). On the other hand, exocytosis did not show an immediate requirement for external Ca^{2+}; increases in C were synchronous with those in G in the absence of Ca^{2+} (Figure 4C, Table I), and increases in C reached almost the same value as those in the presence of Ca^{2+}.

A short delay in the onset of rises in C was sometimes observed at the second application of ACh (Figure 4D, 4−8 s, three out of seven cells). The responses were considerably smaller than those at the first application, presumably due to desensitization of ACh-induced Ca^{2+} signalling in dialysed acinar cells (Marty and Zimmerberg, 1989; Maruyama, 1989b). Thus, rises in G preceded any rises in C during stimulation with both ACh and A23187 (Figure 3A−C). Moreover, rises in C did not *per se* appear to affect G (Figures 3B and C, and 4C). These results indicate that fusion of secretory granules evokes little insertion of active ion channels into the plasma membrane (Iwatsuki and Petersen, 1981), if any (Fuller *et al.*, 1989).

Discussion

The present study experimentally confirmed the reliability of capacitance measurements in exocrine cells, and elucidated clear correlations between temporal patterns of $[Ca^{2+}]_i$ rises and exocytotic secretion. We will further consider each issue in more detail in the following sections.

Reliability in capacitance measurement in exocrine cells

We have demonstrated that the errors in the estimates of C due to changes in G are less than one-tenth of the observed changes in C induced with ACh or A23187 (Figures 2−4).

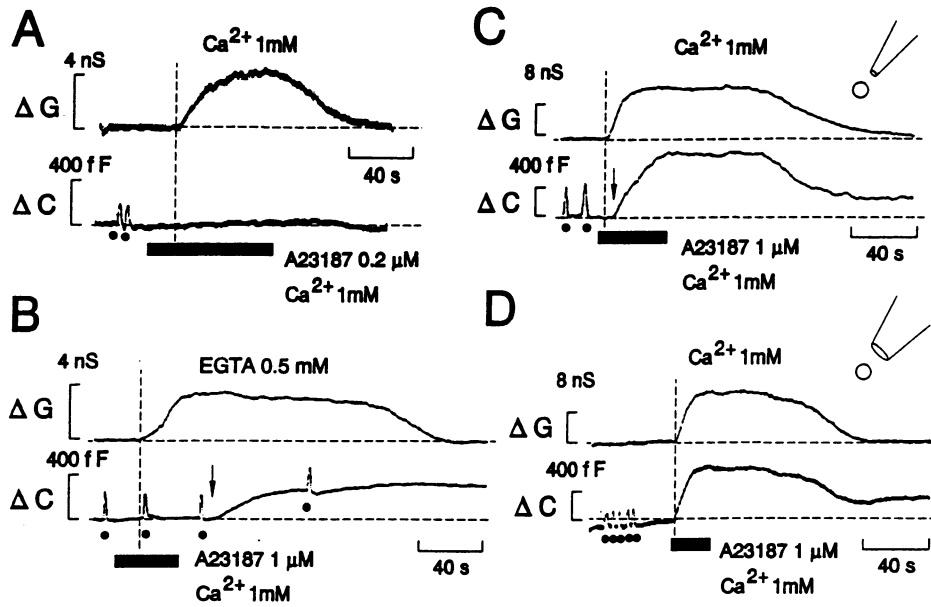

Fig. 3. Changes in C and G in single pancreatic acinar cells induced with A23187. (**A**) Effects of a low concentration (0.2 μM) of A23187. (**B**) Effects of a high concentration (1 μM) of A23187 together with 1 mM Ca^{2+} examined in a cell immersed in a Ca^{2+}-free solution containing 0.5 mM EGTA for 10 min. (**C**) Effects of 1 μM of A23187 in the presence of Ca^{2+}. Arrows in (B) and (C) indicate the onset of rises in C. (**D**) Effects of 1 μM A23187 in another cell, where A23187 was applied using a pipette with a large orifice (30 μm) as illustrated in the inset. Open circles in the insets in (C) and (D) represent the size of acinar cells. Vertical dotted lines represent the onsets of rises in G. Filled circles underneath ΔC traces are calibration signals with an amplitude of 200 fF in (A), (B) and (D), and of 400 fF in (C).

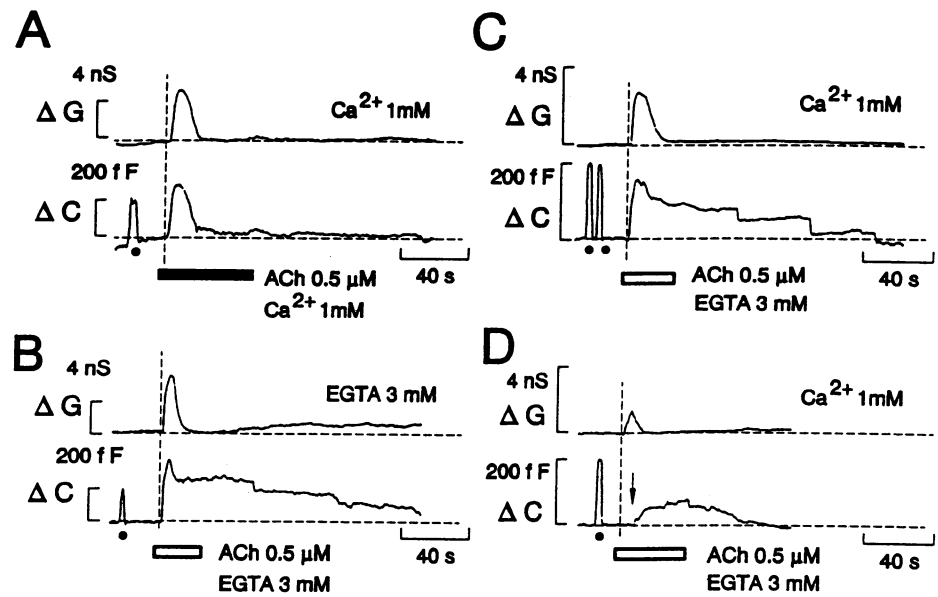

Fig. 4. Changes in C and G induced by ACh (0.5 μM). (**A**) and (**B**) Effects of ACh in the presence (A) or absence (B) of external Ca^{2+}, studied in two different cells. (**C**) and (**D**) Effects of ACh applied together with EGTA (3 mM) twice on the same cell: (C) shows the response at the first application and (D) at the second application. An arrow indicates the onset of rises in C. Filled circles below ΔC traces show ΔC of 200 fF.

Indeed, clear dissociation of ΔC and ΔG was found in three different experimental conditions. First, recovery from rises in C was retarded in the absence of external Ca^{2+} (Figures 3B and 4B). Second, the onset of changes in C was delayed relative to changes in G when cells were stimulated with A23187 (Figure 3B and C) or with a second application of ACh (Figure 4C). Third, selective increases in G were induced with a low concentration of A23187 (Figure 4A).

Observed errors could be predicted well by theoretical analysis. Errors in the estimates of C (EC_{error}) due to a change in G (Δ) could be approximated by

$$EC_{error}(\Delta G) = \theta \frac{\Delta G}{\omega} + C \frac{\Delta G^2}{Gs^2}, \qquad (1)$$

where Gs represents access resistance, ω the frequency of the sine wave applied to the voltage command, and θ the

error in the adjustment of phase offset (see Materials and methods for derivation of equation 1). Given the typical values for C, Gs and ω of 10 pF, 10 MΩ and 1884, respectively, the predicted errors calculated using equation 1 are as plotted with dotted lines in Figure 1B at several different values of θ. When values of θ are between -0.02 and -0.03, the prediction could well explain the observed linear relationship between ΔG and ΔC as well as a sign of saturation at larger values of ΔG (Figure 1B). The reason why θ tended to have small negative values in actual experiments is mentioned in Materials and methods. Thus, we believe that the capacitance measurement gives good estimates of actual changes in capacitance even when they are accompanied by a certain amount of change in G.

Ca^{2+} spikes and exocytotic secretion in the exocrine gland

We believe our results indicate that exocytotic fusion is less sensitive to Ca^{2+} than Ca^{2+}-dependent ion channels: a low concentration (0.2 μM) of A23187 caused rises in G without affecting C. The level of $[Ca^{2+}]_i$ necessary for inducing exocytotic fusion is probably >0.3 μM, because 0.2 μM A23187 homogeneously raised $[Ca^{2+}]_i$ to 0.3 μM (Table I). On the other hand, 0.3 μM $[Ca^{2+}]_i$ activates ion channels. Assuming the threshold $[Ca^{2+}]_i$ levels for the ion channels and exocytotic fusion to be 0.2 and 0.4 μM, respectively, time lags between rises in G and C induced with A23187 fit well with observed time lags for $[Ca^{2+}]_i$ to rise from 0.2 to 0.4 μM (Table I).

We found no delay in C relative to G with ACh stimulation (Figure 4A–C, Table I). This fits qualitatively with the observed ACh-induced rapid rises in $[Ca^{2+}]_i$ at the granular area (Figure 1B). The rapid onset of C synchronous to G indicates that exocytotic secretion was triggered with the localized Ca^{2+} spikes by themselves, because we know that rapid onset of increases in G are associated temporally with localized Ca^{2+} spikes at the granular area (Kasai and Augustine, 1990). More quantitatively, however, rises in $[Ca^{2+}]_i$ were not so rapid as to account for the lack of lag between G and C: there were lags in $[Ca^{2+}]_i$ increases (0.4 s, Table I). This is particularly noteworthy, since we were using a confocal microscope to measure $[Ca^{2+}]_i$ confined to the granular area. We suggest that the rapidity in the effect of ACh could be explained by more rapid and more spatially restricted rises in $[Ca^{2+}]_i$ around the secretory granules than could be detected with a confocal microscope. Even A23187 could elicit rapid rises in C when it was applied sufficiently fast (Figure 3D). It is interesting to note that rises in Ca^{2+} which lead to vesicle fusion may be mediated by Ca^{2+} release from organelles in the granular area (Marty, 1991). In fact, increases in $[Ca^{2+}]_i$ always started at the granular area where secretory granules lie (Kasai and Augustine, 1990; Nathanson *et al.*, 1992; Tan *et al.* 1992; Toescu *et al.*, 1992). If so, the rapid occurrence of secretion could be explained by the large rises in $[Ca^{2+}]_i$ formed just outside the open Ca^{2+} release channels close to the secretory granules. Thus, the regulation of secretion in exocrine gland cells by Ca^{2+} might share a similarity with neurotransmitter release (Smith and Augustine, 1988), in that both may utilize large $[Ca^{2+}]_i$ rises close to the open Ca^{2+} channels.

Our study demonstrated that exocytotic secretion could be triggered directly by individual Ca^{2+} spikes, because exocytotic fusion was less sensitive to Ca^{2+}, and because Ca^{2+} spikes were sufficient for triggering exocytotic fusion. In exocrine cells, agonists trigger repetitive Ca^{2+} spikes, known as Ca^{2+} oscillation (Maruyama, 1988; Petersen, 1992). Our study, therefore, suggests that exocytotic secretion is triggered in phase with oscillatory Ca^{2+} rises even during tonic stimulation. This mechanism offers a precise and noise-resistant way of translating the concentration of agonists into an appropriate amount of secretion.

Materials and methods

Preparation of single pancreatic acinar cells

Male Wistar rats (6–10 weeks old) were sacrificed by cervical dislocation, and a small piece of pancreas or lacrimal gland was excised. The glands were dissociated into single acinar cells using a serial enzymatic treatment first with collagenase (200 U/ml, Wako, Tokyo) for 6 min, then with trypsin (0.5 mg/ml, Sigma type XI, St Louis, MO) for 4 min and finally with collagenase for 3 min (Maruyama, 1990). The enzymatic treatments were carried out at 36°C in a solution composed of 113 mM NaCl, 4.7 mM KCl, 2.56 mM $CaCl_2$, 1.13 mM $MgCl_2$, 2.8 mM glucose, 4.9 mM sodium pyruvate, 2.7 mM sodium fumarate, 2.7 mM sodium glutamate, 25 mM Na-HEPES at pH 7.3 and 2 g/l bovine serum albumin. The dispersed acinar cells were plated in a solution containing 145 mM NaCl, 4 mM KCl, 1 mM $CaCl_2$, 2 mM $MgCl_2$, 10 mM Na-HEPES at pH 7.3. Physiological experiments were performed within 1.5 h after dissociation of cells at room temperature (22–25°C).

Ca^{2+} imaging with a confocal laser microscope

The dissociated cells were loaded with an acetoxymethyl form of a Ca^{2+} indicator dye, fura red (10 μM, Molecular Probes), for 30 min at room temperature. Fluorescence from acinar cells was detected with a confocal laser scanning microscope (Bio-Rad, MRC-600) attached to an inverted microscope (Olympus, IMT-2) with a 60×, n.a. = 1.3, oil immersion objective. An argon laser was used to excite fura red at 512 nm. The fluorescence of fura red decreases when $[Ca^{2+}]_i$ increases. The ratio of the maximal fluorescence to the minimum (F_{max}/F_{min}) was estimated as 5.1 and the affinity to Ca^{2+} (K_d) as 0.15 μM, using small droplets of intracellular solutions whose Ca^{2+} had been chelated to known values with EGTA (Neher, 1988). $[Ca^{2+}]_i$ was obtained by taking the ratio of fluorescence value during stimulation (F) to that before stimulation (F_o), as $[Ca^{2+}]_i = (a \cdot K_d - K_d')/(1 - a)$, where $a = b \cdot F/F_o$, $K_d' = K_d \cdot F_{max}/F_{min}$, $b = ([Ca^{2+}]_{i,0} + K_d')/([Ca^{2+}]_{i,0} + K_d)$, and $[Ca^{2+}]_{i,0}$ resting $[Ca^{2+}]_i$. We assumed $[Ca^{2+}]_{i,0}$ to be 0.1 μM and that there was no resting $[Ca^{2+}]_i$ gradient (Toescu *et al.*, 1992). Two-dimensional images composed of 128 × 128 pixels were acquired every 0.75 s. $[Ca^{2+}]_i$ levels were represented in a pseudocolour code. A Ca^{2+}-ionophore, A23187, (0.5–1 μM) and acetylcholine (ACh, 0.5–1 μM) were applied on to the cell from a glass pipette (ϕ = 4 μm) positioned within 10 μm of the cell with positive pressures (1–2 m H_2O), unless otherwise stated.

Patch-clamp experiments

Current responses were recorded with the standard whole-cell patch-clamp technique (Hamill *et al.*, 1981). Patch pipettes were coated with Sylgard resin and filled with a solution containing 148 mM potassium glutamate, 2 mM $MgCl_2$, 1 mM Na_2-ATP, 0.5 mM EGTA, 0.178 mM $CaCl_2$, 10 mM K-HEPES, at pH 7.2 and pCa 7. For the experiments using the lacrimal gland cells, patch pipettes contained 3 mM EGTA. Resistances of the patch pipettes filled with these solutions ranged from 2 to 5 MΩ. Simultaneous measurements of changes in capacitance (C) and conductance (G) were performed in the whole-cell recording mode using a patch-clamp amplifier (EPC-7, List, Darmstadt) and a two-phase lock-in amplifier (NF5610B, NF Instruments, Yokohama), as described previously (Neher and Marty, 1984; Lindau and Neher, 1988; Maruyama, 1988). Briefly, the capacitive transients originating from the capacitance of plasma membranes were minimized by adjusting the capacitance and time constant of a capacitance cancellation circuit in the patch-clamp amplifier while applying voltage pulses with an amplitude of 10 mV. This adjustment gave whole-cell capacitance values of 9–11 pA and series resistance values of 5–12 MΩ. After the cancellation, we applied a sine wave to voltage command. The sine wave had a frequency of 300 Hz and an amplitude of 10 mV, and was given

at a holding potential of −40 mV. The resultant current output was fed into the lock-in amplifier. The phase offset of the lock-in amplifier was adjusted so that when the capacitance of the cancellation circuit was modified in order to calibrate C, there was no change in the output for G (circles at ΔC traces in Figures 2−4).

Theoretical evaluation of the error in the estimates of ΔC due to ΔG

Following the notations used in Neher and Marty (Neher and Marty, 1984), the admittance (Y) of the model circuit of the whole-cell recording can be expressed in complex form as

$$Y(G,C) = (G + j\,\omega\,C)\,B(G,C),$$

where ω represents the angular velocity of the sine waves applied to the voltage command, and $B(G,C) = 1/(1 + G/Gs + j\omega C/Gs)$, where Gs represents the access resistance. After correction of the phase offset with a lock-in amplifier, the apparent admittance is expressed as

$$E(G,C) = \frac{Y(G,C)}{B^2(G,C)\,(\cos(\theta) - j\,\sin(\theta))}. \quad (2)$$

Positive values of θ represent over-compensation. Correction of phase offset by $B^2(G,C)$ is considered optimal when changes in G are the major origin of the errors in the estimate of C (Joshi and Fernandez, 1988). The estimates of capacitance and conductance are given by the imaginary and real parts of E(G,C), respectively. Then, the errors in the estimate of C due to ΔG are calculated as

$$EC_{error}(\Delta G) = Im\left(\frac{Y(G+\Delta G,C) - Y(G,C)}{B^2(G,C)\,(\cos(\theta) - j\,\sin(\theta))}\right) =$$

$$\left|B^2(G + \Delta G,C)\right|\left(\frac{\sin(\theta)}{\omega}\left((1 + \frac{G}{Gs})\left(1 + \frac{G+\Delta G}{Gs}\right)\right.\right.$$

$$\left.\left. + \left(\frac{\omega\,C}{Gs}\right)^2\right)\Delta G + \cos(\theta)\,C\left(\frac{\Delta G}{Gs}\right)^2\right).$$

Assuming that θ is small, $G << Gs$, $\Delta G << Gs$, and $\omega C^2 << Gs^2$, equation 3 can be approximated with equation 1.

We next evaluate the error in the phase offset, θ. We adjusted the phase offset so that no change in the estimates of G was detected when 1 pF of ΔC was applied from the capacitance trimmer. Assuming that the trimmer gives precisely the same angle as changes in C provide, the observed changes in the estimates of G due to the change in C are calculated as :

$$EG_{error}(\Delta G) = Re\left(\frac{Y(G,C + \Delta C) - Y(G,C)}{B(G,C)\,(\cos(\theta) - j\,\sin(\theta))}\right) =$$

$$\left|B^2(G+\Delta G,C)\right|\left(-\sin(\theta)\,\omega\,\Delta C\left(\frac{1}{\left|B^2(G+\Delta G,C)\right|}\right) - \left(\frac{\omega\,C}{Gs}\right)^2\right)$$

$$\left. + \cos(\theta)\,\omega^2\,\frac{\Delta C^2}{Gs}\left(1 + \frac{G}{Gs}\right)\right).$$

This could be approximated by the following equation with the same assumptions as above:

$$EG_{error}(\Delta C) = -\theta\omega\Delta C + \frac{\omega^2\Delta C^2}{Gs}. \quad (5)$$

Given that noise level in the estimates of G is smaller than 10 pS and ΔC applied from the capacitance trimmer is 1 pF, $|EG_{error}| < 10$ pS. This yields $|\theta - 0.018| < 0.0053$. Thus, the precision in the estimates of θ could be as high as 0.0053 (0.3°). In actual experiments, values of θ were around −0.025 (−1.4°), as shown in Figure 1B. This may be due to the tendency to under-compensate for the capacitive transients: a small and slow component is always left uncancelled. This causes less-compensated calibration signals for C, and lesser correction of the phase offset. The under-compensation might be good for our experiments; equation 1 indicates that errors due to changes in G are smaller in slightly under-compensated conditions than in over-compensated conditions, because two components in the right side of equation 1 can be cancelled out (Figure 2B).

Acknowledgements

The authors thank Tristan Davies for improving the manuscript. The work was supported by grants-in-aid for scientific research from the Japanese Ministry of Education, Science and Culture to Y.Maruyama, H.K. and Y.Miyashita, and by grants from the Human Frontier Science Program to H.K.

References

Berridge,M. (1993) *Nature*, **361**, 315−325.
Brundage,R.A., Fogarty,K.E., Tuft,R.A. and Fay,F.S. (1991) *Science*, **254**, 703−706.
Findlay,I. (1984) *J. Physiol.*, **350**, 179−195.
Fuller,C.M., Eckhardt,L. and Schultz,I. (1989) *Pflügers Arch.*, **413**, 385−394.
Hamill,O.P., Marty,A., Neher,E., Sakmann,B. and Sigworth,F. (1981) *Pflügers Arch.*, **391**, 85−100.
Iwatsuki,N. and Petersen,O.H. (1981) *J. Physiol.*, **314**, 79−84.
Joshi,C. and Fernandez,J.M. (1988) *Biophys. J.*, **53**, 885−892.
Kasai,H. and Augustine,G.J. (1990) *Nature*, **348**, 735−738.
Lindau,M. and Neher,E. (1988) *Pflügers Arch.*, **411**, 137−146.
Marty,A. (1991) *J. Membr. Biol.*, **124**, 189−197.
Marty,A. and Zimmerberg,J. (1989) *Cell. Signal.*, **1**, 259−268.
Maruyama,Y. (1988) *J. Physiol.*, **406**, 299−313.
Maruyama,Y. (1989a) *Pflügers Arch.*, **413**, 438−440.
Maruyama,Y. (1989b) *J. Physiol.*, **417**, 343−359.
Maruyama,Y. (1989c) *News Physiol. Sci.*, **4**, 53−56.
Maruyama,Y. (1990) *J. Physiol.*, **430**, 471−482.
Nathanson,M., Padfield,P.J., O'Sullivan,A.J., Burgsthler,A.D. and Jamieson,J.D. (1992) *J. Biol. Chem.*, **267**, 18118−18121.
Neher,E. (1988) *J. Physiol.*, **395**, 193−214.
Neher,E. and Marty,A. (1984) *Proc. Natl Acad. Sci. USA*, **79**, 6712−6716.
Petersen,O.H. (1992) *J. Physiol.*, **448**, 1−51.
Smith,S.J. and Augustine,G.J. (1988) *Trends Neurosci.*, **11**, 458−464.
Tan,Y.P., Marty,A. and Trautmann,A.(1992) *Proc. Natl Acad. Sci. USA*, **89**, 11229−11233.
Toescu,E.C., Lawrie,A.M., Petersen,O.H. and Gallacher,D.V. (1992) *EMBO J.*, **11**, 1623−1629.
Tautmann,A. and Marty,A. (1984) *Proc. Natl Acad. Sci. USA*, **81**, 611−615.

Received on April 5, 1993; revised on April 29, 1993